ATLANTIS PRESS

Advances in Engineering Research (AER), volume 102
Second International Conference on
Mechanics, Materials and Structural Engineering (ICMMSE 2017)

Viscoelastic Analysis of Flexible Pavements Embedded with Controlled Low-Strength Material Bases Using Finite Element Method

Wen-Ling Huang[1, a], Her-Yung Wang[1, b], Li-Jeng Huang[1, c]

[1]Department of Civil Engineering, National Kaohsiung University of Applied Sciences, Kaohsiung, 80778, Taiwan, R.O.C.

[a]wlh@kuas.edu.tw, [b]wangho@kuas.edu.tw, [c]ljhuang@kuas.edu.tw

Keywords: CLSM, FEM, Viscoelatic Analysis, Flexible Pavements

Abstract. This paper presents finite element analysis of 4-layered flexible pavements embedded viscoelastic asphalt concrete (AC) top layer and controlled low-strength materials (CLSM) sublayers as well as graded crushed stone subgrades layers. Two-dimensional deformation assumption is employed. Time-dependent stress-strain relations are treated using Laplace transform based on correspondence principle. Collocation method is employed for inversion of Laplace transformed results into time-domain results. A typical layered pavement is analyzed in which relaxation modulus of top viscoelastic asphalt layer is expressed in Prony series. Two kinds of CLSMs, i.e., CLSM-B80/30% and CLSM-B130/30% are compared with graded crushed stones and AC used for base materials. Time-domain responses of vertical displacement, vertical stress and horizontal stress at the bottom of AC layer are compared. The steady state vertical settlements using CLSM bases (B80/30% and B130/30%) are smaller than that using graded crushed stones even considering viscoelastic behavior of asphalt layer and show to be good materials employed as base substitutes for graded crushed stone in flexible pavement design.

Introduction

Flexible pavements have been widely employed in highway engineering for a long time and recently an effective rapid pavement construction had been achieved by using the controlled low strength materials (CLSM) [1, 2]. CLSM is a kind of flowable fill defined as self-compacting cementitious material that is in a flowable state at the initial period of placement and has a specified compressive strength of 1200 psi or less at 28 days or is defined as excavatable if the compressive strength is 300 psi or less at 28 days [3]. The special features of CLSM include: durable, excavatable, erosion-resistant, self-leveling, rapid curing, flowable around confined spacing, wasting material usage and elimination of compaction labors and equipments, etc. The authors also conducted some preliminary studies on engineering properties of CLSM [4] and the numerical analyses on static and free vibration analysis of CLSM bases in flexible pavements [5, 6].

It is well known that asphalt mixtures have special viscoelastic behavior [7]. Its mechanical response exhibits time and rate dependency. Numerical schemes combined with finite element models and Laplace transform method or time-incremental skills have been applied for flexible pavement analysis [8-10].

This study is aimed at viscoelastic analysis of 4-layered flexible pavements using finite element method. The top layer is considered as Hot Mix Asphalt (HMA) which is modeled as viscoelastic materials; while 4 kinds of base materials are employed, i.e., graded crushed stones, CLSM-B80/30%, CLSM-B130/30% and AC. Comparison study is performed on the comparison of time responses of vertical displacement, vertical stress and horizontal stress located at top of base layer.

Finite Element Modeling of 4-Layered Flexible Pavements

The calculation of displacements, stresses and strains caused by vehicles loads in pavements is a difficult task. Finite element methods can be employed for multilayered elastic/viscoelastic analysis based on correspondence principle.

The stress-strain relationship of a viscoelastic material can be expressed as a form of convolution integrals for stress formulation or strain formulation as

$$\sigma(t) = \int_0^t E(t-\tau) \bullet \frac{\partial \varepsilon}{\partial \tau} d\tau = E(t) \otimes \frac{\partial \varepsilon}{\partial t} \tag{1a}$$

$$\varepsilon(t) = \int_0^t D(t-\tau) \bullet \frac{\partial \sigma}{\partial \tau} d\tau = D(t) \otimes \frac{\partial \sigma}{\partial t} \tag{1b}$$

for uniaxial stress state, where *E (t)* is the relaxation modulus, *D(t)* is the creep compliance, *t* is the current time, is a temporal variable starting from the beginning of loading. Taking Laplace transform of Eq. (1) we have

$$\hat{\sigma}(s) = s\hat{E}(s) \bullet \hat{\varepsilon}(s) \tag{2}$$

Thus based on correspondence principle in the theory of linear viscoelaticity we can replace *E* by $s\hat{E}(s)$ in FEM for stiffness formulation in the theory of elasticity.

$$\hat{K}(s)\hat{X}(s) = \hat{F}(s) \tag{3}$$

where, $\hat{X}(s)$ and $\hat{F}(s)$ are systematic nodal displacement vector and force vector, respectively; and the stiffness matrix in the Laplace transformed domain is expressed as

$$\hat{K}(s) = \int_V [B]^T [\hat{D}(s)][B] dV \tag{4}$$

The calculation of displacements, stresses and strains in Laplace transform domain is the same as for elastic analysis.

The relaxation modulus for a viscoelastic material can be expressed as the Prony series

$$E(t) = E_\infty + \sum_{i=1}^{n} E_i \, e^{-t/\rho_i} \tag{5}$$

where, E_∞, E_i, ρ_i are the coefficients of the Prony series and *n* is the number of terms. The Laplace transform of Eq. (4) is

$$\hat{E}(s) = \frac{E_\infty}{s} + \sum_{i=1}^{n} \frac{E_i}{s + 1/\rho_i} \tag{6}$$

Collocation Method for Inversion of Laplace Transform

Because the field variables calculated by the FEM in Laplace transformed domain are all numerical values, analytical inversion of Laplace transform cannot be obtained and suitable numerical scheme for Laplace transform is required. Among various schemes we adopt Schapery collocation method [11] to evaluate the time-domain results from Laplace transform FE numerical results. Using displacement calculation as an example, assume the time-domain result is

$$w(x,y,t) = w_S(x,y) + \sum_{i=1}^{M} a_i \, e^{-b_i t} \tag{7}$$

where, w_S denotes the steady-state value which can be evaluated using initial-value theorem of Laplace transform, a_i, b_i are constants, M the number of collocation points. Choosing *M* points of collocation and setting $b_i = s_i$, $i = 1,2,\cdots,M$, we can solve a_i from

$$[P]\{a\} = \{\hat{W}(s) - \frac{w_S}{s}\} \quad i, j = 1,2,\cdots, M \tag{8}$$

where,

$$[P] = \begin{bmatrix} \frac{1}{s_1 + s_1} & \frac{1}{s_1 + s_2} & \cdots & \frac{1}{s_1 + s_M} \\ \frac{1}{s_2 + s_1} & \frac{1}{s_2 + s_2} & \cdots & \frac{1}{s_2 + s_M} \\ \vdots & \vdots & \ddots & \vdots \\ \frac{1}{s_M + s_1} & \frac{1}{s_M + s_2} & \cdots & \frac{1}{s_M + s_M} \end{bmatrix} \tag{9}$$

Numerical Results

We consider the 4-layered flexible pavement as illusrated in Fig. 1(a). Different materials in base layer along with all the parameters in all profiles are list in Table 1. The material constants for AC, graded crushed stone, compacted soil and natural soil are the same as those employed for typical highway in Taiwan [12]. The material constants for CLSM-B80/30% and CLSM-B130/30% are obtained from experimental works as explained in [13]. Selection of materials for the CLSM mixture in this study consisted of fine aggregate, type I Portland cement, stainless steel reducing slag (SSRS), and water. Viscoelastic material properties in Prony series of the HMA layer is obtained from [14] as shown in Table 2. The vertical concentrated axle load, $Q_0 = 80\ kN$ (18000 *lbs.* for moment) is assumed. This is equivalent single axle load a common AASHTO HS20 truck.

Table 1. Material Properties and Vertical Model Dimensions.

Layer #	Materials	Thickness (*mm*)	*E* (*MPa*)	ν
1 (Surface)	HMA	100	Eq. (5)	0.35
2 (Base)	Graded Crushed Stone CLSM-B80/30% CLSM-B130/30% AC	500	172 270 870 2069	0.40 0.25 0.25 0.35
3 (Sub-grade)	Compacted Soil	300	138	0.45
4(Sub-grade)	Natural Soil	300	55	0.45

Table 2. Viscoelastic material properties in Prony series of the HMA layer (after Lee, 1996).

i	E_1 (MPa)	ρ_i	D_i $(1/MPa)$	T_i
∞	1.172	-	6.89E-5	-
1	3100	2.20 E-5	9.61E-6	5.00E-6
2	4310	2.20E-4	1.63E-5	5.00E-5
3	3460	2.20E-3	4.92E-5	5.00E-4
4	2020	2.20E-2	1.12E-4	5.00E-3
5	1270	2.20E-1	2.26E-4	5.00E-2
6	272	2.20E+0	5.75E-4	5.00E-1
7	65.9	2.20E+1	3.53E-3	5.00E+0
8	14.5	2.20E+2	8.91E-3	5.00E+1
9	1.52	2.20E+3	6.24E-2	5.00E+2
10	0.710	2.20E+4	3.85E-1	5.00E+3
11	0.0588	2.20E+5	3.92E-1	5.00E+4

The *Q4* finite elements are employed for the displacement and stress analysis, the formulation for the problem can be expressed in matrix form as [15]. Boundary conditions are: hinge supports along *AB*, *BC*, *CD*. For the longitudinal section analyses, totally $30 \times 24 = 720$ rectangular elements along with $31 \times 25 = 775$ nodes are employed for numerical calculation using program coded in MATLAB (Fig. 1(b)).

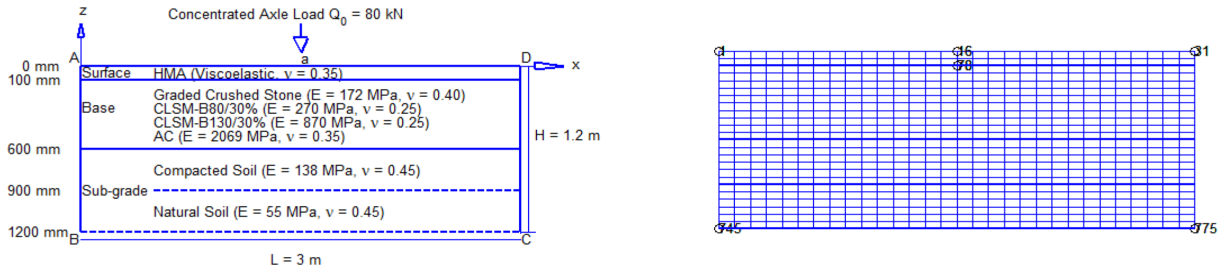

(a) Schematic of 4-layered flexible pavement (b) FEM mesh of 4-layered flexible pavement

Fig. 1 Schematic and FE mesh of 4-layered flexible pavement.

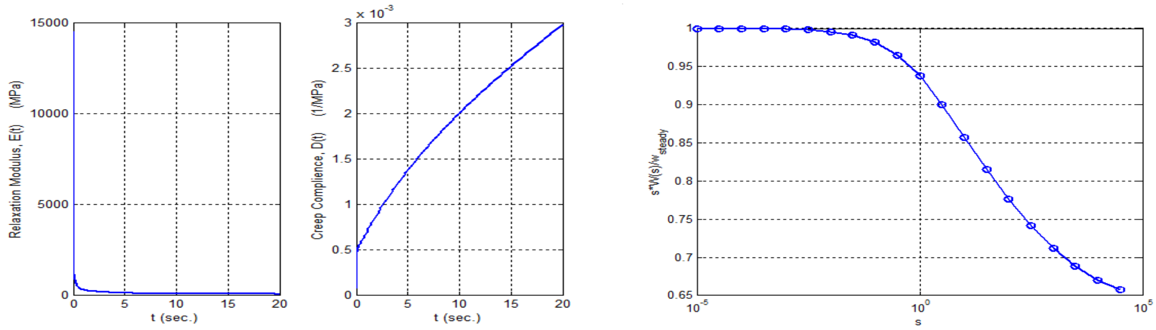

(a) Relaxation modulus and creep compliance; (b) collocation points in s-domain

Fig. 2 Numerical results for viscoelastic flexible pavement.

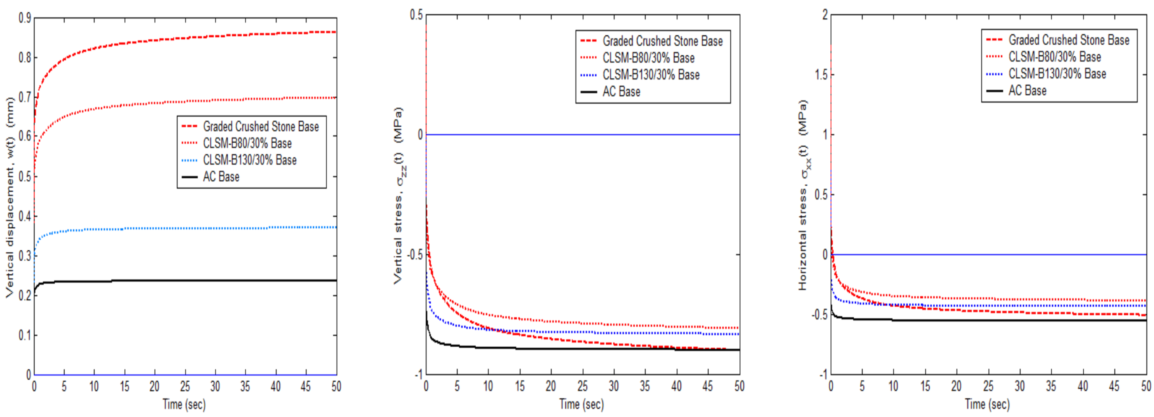

(a) Vertical displacement (b) Vertical stress (c) Horizontal stress

Fig. 3 Time-domain results of displacements and stress of 4-layered flexible pavement.

The relaxation modulus and creep compliance of HMA variation with time are shown in Fig. 2(a). Twenty collocation points employed for calculation of results in Laplace transformed domain are shown in Fig. 2(b). The time-domain results for vertical displacement, vertical stress and horizontal stress located at $(x, z) = (1.5m, -0.1m)$ (i.e., the node 78) are shown in Fig. 3(a), 3(b) and 3(c), respectively. We can observe that the more stiffened the base material employed, the less retardation time for the vertical displacement reaches its steady state values. Furthermore, vertical and horizontal stress relaxations depict approximately the same behavior and order of magnitude for using 4 kinds of base materials. We can realize that the steady state vertical settlements using CLSM bases (B80/30% and B130/30%) are smaller than that using graded crushed stones even considering viscoelastic behavior of top asphalt layer.

Conclusion

Finite element analyses of 4-layered flexible pavements with viscoelastic surface layer embedded with four different base materials analyzed using correspondence principle and collocation method of Laplace transform show that vertical displacement responses at top base layer using CLSMs are bounded by those using graded crushed stone base and AC base. The steady state vertical settlements using CLSM bases (B80/30% and B130/30%) are smaller than that using graded crushed stones even considering viscoelastic behavior of asphalt layer and show to be good materials employed as base substitutes for graded crushed stone in flexible pavement design.

References

[1] D. F. Lin, H. L. Luo, H. Y. Wang, M. J. Hung, Successful Application of CLSM on a Weak Pavement Base/Subgrade for Heavy Truck Traffic, Perform. Constr. Facil. 21(1) (2007) 70-77.

[2] M. Bassani, S. Khosravifar, D. G. Goulias, C. W. Schwartz, Long-term Resilient and Permanent Deformation Behavior of Controlled Low-Strength Materials for Pavement Applications, Transport. Geotech. 2 (2015) 108-118.

[3] ACI-229R, Controlled Low-Strength Materials (Reproved 2005), Farmington Hills (MI) 2005.

[4] L. J. Huang, Y. N. Sheen, D. H. Le, On the Multiple Linear Regression and Artificial Neural Networks for Strength Prediction of Soil-Based Controlled Low-Strength Material, 3rd International Conference for Advanced Materials Design and Mechanics and Workshop on Android Robotics, Singapore, May 23-24, 2014.

[5] L. J. Huang, H. Y. Wang, W. L. Huang, M. C. Lin, Finite Element Analysis of Controlled Low-Strength Material Bases Part I- Static Analysis, ISEC-9, Resilient Structures and Sustainable Construction, Valencia, Spain, 24th-29th, July, 2017 (Accepted).

[6] L. J. Huang, H. Y. Wang, W. L. Huang, M. C. Lin, Finite Element Analysis of Controlled Low-Strength Material Bases Part II- Free Vibration Analysis, ISEC-9, Resilient Structures and Sustainable Construction, Valencia, Spain, 24th-29th, July, 2017 (Accepted).

[7] Y. H. Huang, Pavement Analysis and Design, Prentice-Hall, Inc., 1993.

[8] E. J. Francisco, P. J. Evandro, B. S. Jorge, Viscoelastic and Elastic Structural Analysis of Flexible Pavements, CILAMCE 2005-ABMEC & AMC, Guarapart, Espirto Santo, Brazil, 19th-21th October 2005.

[9] M. Mahmood, A. Mahmoud, M. Parviz, Incremental Layerwise Finite Element Formulation for Viscoelastic Response of Multilayered Pavements, Int. Transp. Eng. 1(3) 2014.

[10] V. D. Eshan, H. P. Glaucio, G. B. William, Viscoelastic Functionally Graded Finite-Element Method Using Correspondence Principle, Mater. Civil Eng. 39-48, January 2011.

[11] R. A. Schapery, Method of Viscoelastic Analysis Using Elastic Solutions, Franklin Inst. 279(4) (1965) 268-289.

[12] D. W. Chang, C. E. Chang, Study on Data Interpretation and Structural Index of Flexible Pavement, Tamkang J. Sci. Eng. 1(2) (1998) 83-96.

[13] Y. N. Sheen, L. J. Huang, D. H. Le, Engineering Properties of Controlled Low-Strength Material Made with Residual Soil and Class F Fly Ash, 3rd International Conference for Advanced Materials Design and Mechanics and Workshop on Android Robotics, Singapore, May 23-24, 2014.

[14] H. J. Lee, Uniaxial Constitutive Modeling of Asphalt Concrete Using Viscoelasticity and Continuum Damage Modeling, PhD Dissertation, Department of Civil Engineering, North Caroline State University, Raleigh, NC, USA, 1996.

[15] D. L. Logan, A First Course in the Finite Element Method, Cengage Learning, 2012.